Research Article

Biao Yang*, Zhaogang Wu, Hao Gao, Liexing Zhou, and Jun Sun

Research on the optimisation of the temperature field distribution of a multi microwave source agent system based on group consistency

https://doi.org/10.1515/htmp-2022-0250
received July 21, 2022; accepted November 02, 2022

Abstract: Aiming at the problem of optimising the temperature field distribution of a multi microwave source agent system, in this work, group consistency is used to explore the multi microwave source agent collaborative tracking strategy to improve both the uniformity of the temperature distribution and the heating efficiency. First, to coordinate the inputting power state information of the multi microwave source agents, a consistency algorithm of non-fully connected communication topology is adopted. Second, according to the efficiency state information of the microwave source agents in different distribution positions of the cavity, the agent group consistency strategy and the group consistency strategy with expected power deviation are used to adjust the power distribution of each agent. Finally, the feasibility and effectiveness of the proposed strategy are verified by using heating materials with different specifications. The experimental results show that compared with the traditional multisource heating method the proposed temperature distribution optimization strategy based on group consistency can improve the temperature uniformity and heating efficiency.

Keywords: multi microwave source agent, expected state deviation, agent group, group consistency, collaborative optimisation

*** Corresponding author: Biao Yang,** Faculty of Information Engineering and Automation, Kunming University of Science and Technology, Kunming, 650500, China; Key Laboratory of Unconventional Metallurgy of Ministry of Education, Kunming University of Science and Technology, Kunming, 650093, China; Yunnan Key Laboratory of Artificial Intelligence, Kunming University of Science and Technology, Kunming, Yunnan, 650500, China, e-mail: biaoykmust@kust.edu.cn
Zhaogang Wu, Hao Gao, Liexing Zhou, Jun Sun: Faculty of Information Engineering and Automation, Kunming University of Science and Technology, Kunming, 650500, China

Nomenclature

a_{ij}	elements of adjacency matrix
A_1, A_2, A_m, A_{m1}	curve amplitude
A_n	adjacency matrix
B	magnetic induction intensity
c_0	speed of light in vacuum
C_p	specific heat capacity
E	electric field intensity
E_n	set of edges formed by ordered node pairs in V_n
G_n	directed graph
h	heat transfer coefficient of air
H	magnetic field intensity
k_0	wavenumber in free space
k	thermal conductivity
K_r, γ, λ	weight vector
i	number of each agent
L_n	Laplacian matrix
n	unit normal vector
$P(\tau)$	total incoming power
P_{in}	total energy fed into reaction chamber
$P_i(\tau)$	the power curve of the ith microwave source agents with time τ as the independent variable
P_r	reflected power
Q	microwave dissipation power
Q_e	dielectric loss
Q_m	hysteresis loss
q	heat flux
$Q_e(\tau)$	the electromagnetic power loss density at time τ
ε_0	vacuum dielectric constant of medium
ε_r	relative permittivity of medium
μ_0	vacuum permeability
μ_r	relative permeability of medium
ω	angular frequency of incident electromagnetic wave
t	time
T	temperature

T_{air}	temperature of air medium in the chamber
T_a	average temperature of the selected area
T_0	initial temperature
u	control information input
u_i	control information input of each agent
V_n	finite set of non-empty nodes
ε''	imaginary part of dielectric constant
μ''	imaginary part of permeability
ρ	density of medium
ξ^r, ξ_r'	leader status information
$\Delta_{ij} = \delta_i - \delta_j$	difference of expected information state
$\dot{\xi}^r$, $\dot{\xi}_r'$	derivative of leader state
$\Delta_{ij} = \varsigma_i - \varsigma_j$	difference of expected information state
$\partial T/\partial n$	temperature gradient perpendicular to the surface of the temperature domain
ξ_0	initial value of agent output power
φ	phase difference
ΔT	average temperature rise
ξ	status information of solid-state microwave source
ξ_0^r	curve amplitude

1 Introduction

Microwave heating has the advantages of high efficiency, selectivity, and noncontact and control without hysteresis [1]. As a clean new heating method, it has been widely used in daily life and for industrial heating [2]. However, the complex internal heat generation mechanism of microwave heating, random hot-spot generations, and difficult mathematical model make it difficult to accurately obtain and optimise the temperature distribution [3]. Furthermore, the uneven temperature distribution and low efficiency of energy use problems in the microwave heating process also need special attention.

Research studies on improving the temperature uniformity of heated materials in the microwave heating process can be divided into two categories. The first category is focused on optimising the design of the microwave reaction cavity to change the electromagnetic field distribution in the cavity or to use a moving object to change the absorption of microwaves to improve temperature uniformity. In this regard, Plaza-Gonzalez et al. added several mode agitator configurations to the cavity to improve the uniformity of the electric field [4]. Wu et al. designed an accordion microwave cavity, and the geometry of the cavity was reconstructed during microwave heating [5]. In other studies, a rotary table was added into the cavity to avoid continuous heating at a fixed position by continuously rotating the heating material [6,7]. Furthermore, scholars have also expanded this approach, for example, Meng et al. studied the influence of metal points embedded in a turntable on heating uniformity, and the results showed that the rotating metal points can considerably improve the heating uniformity and efficiency [8]. Ye et al. divided the turntable into two parts using different materials, studied the combination of three different materials, and found that the turntable composed of multiple materials can improve the uniformity by 26–47% compared with a single material turntable [9]. Liao et al. designed a deformable cavity structure with a slider, which improved heating uniformity by using the phase shift method [10]. Zhu et al. developed a rotating radiation waveguide to improve the heating uniformity by optimising the rotation angle [11]. Zhao et al. studied the addition of bubbles in heated material. Compared with the absence of bubbles in a reactor, the bubbles substantially improved the temperature uniformity [12].

The second category is focused on microwave sources, such as variable frequency microwave (VFM) technology [13], phase-shifting techniques [14], pulsed microwave sources, or the use of multiple microwave sources. Using multiple microwave sources can improve the uniformity by improving the distribution of the electromagnetic field in the cavity. Boonthum et al. developed a four source microwave reactor, that can heat SiC to 1,000°C in a few minutes [15]. He et al. studied a rotating waveguide structure and used the gradient descent algorithm to optimise the heating time of the waveguide at different angles, which can considerably improve the heating uniformity [16]. Xiong et al. studied the effects of dual frequencies and pins on temperature uniformity and heating efficiency [17]. Ahn and Lee proposed a waveguide containing vertical and horizontal slit arrays to feed microwaves. Its function is similar to multisource heating. Compared with traditional microwave heating equipment, this device can greatly improve the heating uniformity [18]. At the same time, considering the limited power of a single microwave source and the need for multiple microwave sources in modern industrial high-power microwave heating equipment, there are requirements for the consistency of the output power of multiple microwave sources.

With the development of artificial intelligence, many innovative algorithms for solving optimisation problems have emerged [19,20] or deep learning methods have been used to diagnose [21] and classify various problems [22]. Among them, the multiagent problem is one of them. Due to the wide application of multiagent systems in many fields, such as satellite communications, robot formation

and biological systems, the consistency of multiagent systems is a hotspot of collaborative control research. Wang proposed a distributed control algorithm where a single agent only uses local information under the general directed graph to solve the consistency control problem of high-order nonlinear multiagent systems with unknown control direction in the leaderless state [23]. Li et al. proposed a multiagent consistency control algorithm with a predictable leader trajectory, which transforms the leader-follower consistency problem into a finite/infinite linear quadratic regulator problem [24]. Wu et al. also proposed a distributed packet consistency algorithm with communication delay under time-varying topology for heterogeneous multiagent systems based on algebraic graph theory [25]. Wang et al. presented an effective distributed impulse traction control strategy that realises the global and exponential consistency of the leader-following consistency problem of nonlinear multiagent systems with general time-varying delay and distributed time-varying delay [26]. Yang et al. proposed an intelligentization design scheme of each microwave source in the process of multisource microwave heating, and a new numerical calculation model of multisource coordinated heating was constructed. Compared with the traditional single source heating model, this scheme improves the temperature uniformity, but the heating efficiency is not considerably improved, and the energy utilisation rate is limited [27].

The objective of this study is to improve both the temperature uniformity and heating efficiency of a multi microwave source agent system. Due to complex characteristics such as the strong coupling of multiphysics fields and the heterogeneity of the heated material, it is difficult to directly optimise the uniformity of the temperature distribution. Therefore, the idea of indirect control is adopted in this study. The innovation lies in the following:

(1) Based on the intellectualisation of microwave sources in the process of multisource microwave heating, from the perspective of optimising the electromagnetic field distribution in the reaction cavity and considering the output characteristics of solid-state sources, the consistency algorithm based on algebraic graph theory is applied to realise the coordinated output of the power of multiple microwave sources.
(2) Using the self-organising characteristics of the temperature distribution in the heated material, the power is slowly reduced while ensuring that the overall average temperature continues to rise, making the hot spot temperature conduct to the relatively low-temperature area to enhance temperature uniformity.
(3) Furthermore, to improve heating efficiency, according to the different heating efficiencies when the microwave source agents are distributed in different positions of the cavity, the multi microwave source agents are grouped, and different groups of agents track various power curves. To improve the heating efficiency, a consistency algorithm with an expected state deviation is introduced to facilitate the convergence of different agents to a consistent state according to their different needs, and a new multi microwave source agent cooperative with consistent heating numerical calculation model is constructed.

Because the use of complex control algorithms to directly control and optimise temperature uniformity is not conducive to practicality, the indirect control method proposed in this study is simpler and more practical and has more contribution value in engineering implementation. The results show that the new microwave heating model constructed in this work with multi microwave source intelligent body variable power cooperative output can effectively improve the temperature uniformity and the heating efficiency compared with the traditional microwave heating model.

2 Preparatory knowledge

2.1 Microwave heating calculation process

The electric field distribution in a microwave reaction cavity can be obtained by solving the Maxwell waveform equation as follows [28,29]:

$$\nabla \times \mu_r^{-1}(\nabla \times \boldsymbol{E}) = k_0^2\left(\varepsilon_r - \frac{j\sigma}{\omega\varepsilon_0}\right)\boldsymbol{E}, \tag{1}$$

$$k_0 = \omega\sqrt{\varepsilon_0\mu_0} = \frac{\omega}{c_0}, \tag{2}$$

where ε_0 and ε_r denote the vacuum permittivity and relative permittivity of the medium, respectively; μ_0 and μ_r denote the vacuum permeability and relative permeability of the medium, respectively; $\boldsymbol{E}$ is the electric field intensity; ω is the angular frequency of the incident electromagnetic wave; c_0 is the speed of light in vacuum ($\mathrm{m{\cdot}s^{-1}}$); and k_0 denotes the wavenumber in free space.

In the process of microwave heating, heat is generated by both the dielectric loss Q_e and the hysteresis loss Q_m of the material:

$$Q = Q_e + Q_m = \frac{1}{2}\omega\varepsilon_0\varepsilon''|\boldsymbol{E}|^2 + \frac{1}{2}\omega\mu_0\mu''|\boldsymbol{H}|^2, \tag{3}$$

where Q denotes the microwave dissipation power, Q_e denotes the dielectric loss, Q_m denotes the hysteresis loss, $\boldsymbol{H}$ denotes the magnetic field strength, and ε'' and μ'' denote the imaginary parts of the dielectric constant and magnetic permeability, respectively.

The heating process is accompanied by solid heat conduction, and the temperature of the heated material can be solved by the heat conduction in equation (4) as follows:

$$\rho C_p \frac{\partial T}{\partial t} - k\nabla^2 T = Q, \tag{4}$$

where T is the temperature, ρ represents the density of the medium, C_p is the specific heat capacity, and k is the thermal conductivity.

When the material does not exhibit obvious magnetisation during heating, the heat is mainly converted from dielectric loss, and the hysteresis loss can be ignored:

$$\rho C_p \frac{\partial T}{\partial t} - k\nabla^2 T = \frac{1}{2}\omega\varepsilon_0\varepsilon''|\boldsymbol{E}|^2. \tag{5}$$

According to equation (5), when the heated material remains unchanged, its temperature distribution can be adjusted by adjusting the power to adjust the distribution of the electric field intensity $\boldsymbol{E}$ and electromagnetic wave angular frequency ω.

2.2 Consistency algorithm

2.2.1 Basic consistency theory

In the multiagent system, the directed graph and undirected graph in graph theory are used to represent the relationship between multiple agents from a mathematical perspective. We define a directed graph $G_n \triangleq (V_n, E_n)$, where $V_n = \{1,2,\ldots,n\}$ is a finite set of non-empty nodes and E_n is the set of edges consisting of ordered pairs of nodes in V_n, that is, $E_n \subseteq V_n \times V_n$. An edge (i, j) in E_n indicates that the agent can obtain information from the agent, but not vice versa. A directed graph is a sequence of edges of the form $(i_1, i_2), (i_2, i_3), \ldots$ is a directed path. In a directed graph, a circle indicates that a directed path starts and ends at the same node. If every point in the graph can find a path to any other point, the graph is a connected graph, and a connected acyclic graph is called a tree. If $V_n^s \subseteq V_n$, $E_n^s \subseteq E_n \cap (V_n^s \times V_n^s)$, then $G_n^s(V_n^s \times V_n^s)$ is a subgraph of $G_n(V_n, E_n)$. When the subgraph G_n^s is a directed spanning tree and $V_n^s = V_n$, then G_n^s is a directed spanning tree of G_n.

In applications, adjacency matrices are often used to represent graphs algebraically. Therefore, we define an adjacency matrix $A_n = [a_{ij}] \in R^{n\times n}$, where when $(i, j) \in E$, a_{ij} is a positive weight, otherwise $a_{ij} = 0$. We define a Laplace matrix as $L_n = [l_{ij}] \in R^{n\times n}$, where $l_{ii} = \sum_{j=1, j\neq i}^{n} a_{ij}$, $l_{ij} = -a_{ij}$, $i \neq j$.

The control characteristics of a solid-state microwave source can be regarded as a first-order control system. In continuous time, the state characteristics of the multisource microwave power output can be described as follows:

$$\dot{\xi}_i = u_i, \quad i = 1, \ldots, n, \tag{6}$$

where ξ is the status information of the solid-state microwave source, that is, the output power value. u is the control information input, and i is the number of each agent. u_i is the control information input of each agent.

The whole agent system tracks the ideal power curve, uses the leader-follower strategy, and introduces a virtual leader. Ref. [30] provides a consistency algorithm for a leader's nonfully connected fixed topology:

$$\begin{aligned} u_i = {} & \frac{1}{k_i}\sum_{j=1}^{n} a_{ij}[\dot{\xi}_j - K_{ri}(\xi_i - \xi_j)] + \frac{1}{k_i} a_{i(n+1)}[\dot{\xi}^r \\ & - K_{ri}(\xi_i - \xi^r)], \end{aligned} \tag{7}$$

where $\frac{1}{k_i} \triangleq \sum_{j=1}^{n+1} a_{ij}$, K_r is the weight vector, ξ^r is the virtual leader state information, and $\dot{\xi}^r$ is the derivative of the leader state. a_{ij} is the element of the adjacency matrix of the topology network, that is, the (i, j) item of the adjacency matrix. After the introduction of the virtual leader, the adjacency matrix needs to be expanded. The nth + 1st row is all zeros, and the nth + 1st column is the connection between the virtual leader and each agent.

Ref. [31] also provides Theorem 1 based on control law (7):

Theorem 1. *When and only when the topology graph G_{n+1} of the leader is introduced, with adjacency matrix $A_{n+1} = [a_{ij}] \in R^{(n+1)\times(n+1)}$ when there is a directed spanning tree and the leader node is the root node, the system uses the control law* (7) *to achieve progressive consistency $\xi_i \to \xi^r$.*

From equations (6) and (7), we have:

$$\begin{aligned} & \sum_{j=1}^{n+1} a_{ij}u_i = \sum_{j=1}^{n} a_{ij}\dot{\xi}_j - K_{ri}\sum_{j=1}^{n} a_{ij}(\xi_i - \xi_j) \\ & - K_{ri}a_{i(n+1)}(\xi_i - \xi^r) + a_{i(n+1)}\dot{\xi}^r \Longleftrightarrow \sum_{j=1}^{n+1} a_{ij}u_i \\ & \quad - \sum_{j=1}^{n} a_{ij}u_j - a_{i(n+1)}\dot{\xi}^r \\ & = -K_{ri}\left[\sum_{j=1}^{n} a_{ij}(\xi_i - \xi_j) + a_{i(n+1)}(\xi_i - \xi^r)\right]. \end{aligned} \tag{8}$$

Converted to matrix form:

$$L_{n\times(n+1)}\bar{u} = -K_r L_{n\times(n+1)}\bar{\xi}, \tag{9}$$

where $\bar{u} \triangleq [u|\dot{\xi}^r]^T = [u_1, \ldots u_n, \dot{\xi}^r]^T$, $\bar{\xi} \triangleq [\xi|\xi^r]^T = [\xi_1, \ldots \xi_n, \xi^r]^T$, $L_{n\times(n+1)}$ is the first n rows of the Laplacian matrix L_{n+1}.

We rewrite $L_{n\times(n+1)}$ as $[M|b]$, that is, $M = L_n$, $b = [-a_{1(n+1)}, \ldots, -a_{n(n+1)}]^T$.

$$Mu + b\dot{\xi}^r = -K_r(M\xi + b\xi^r). \tag{10}$$

When G_{n+1} contains a directed spanning tree, the rank of L_{n+1} is n, and the last row of L_{n+1} is all 0, so M is full of rank. Additionally, the n + 1st column of L_{n+1} can be determined by the first n columns, i.e., $b = -M1_n$. Then there are

$$u - 1_n\dot{\xi}^r = -K_r(\xi - 1_n\xi^r). \tag{11}$$

Let $\sigma = \xi - 1_n\xi^r$; then, we have

$$\dot{\sigma} = -K_r\sigma. \tag{12}$$

By equation (12), when $t \longrightarrow \infty$, $\xi_i \longrightarrow \xi^r$.

2.2.2 Consistency with fixed expected state deviation

The time-varying consistency algorithm with relative deviation [31] is introduced to coordinate the output power state of each microwave source agent.

$$\begin{aligned} u_i = \dot{\delta}_i + \frac{1}{\eta_i}\sum_{j=1}^{n} a_{ij}\{\dot{\xi}_j - \dot{\delta}_j - \gamma[(\xi_i - \xi_j) - (\delta_i - \delta_j)]\} \\ + \frac{1}{\eta_i}a_{i(n+1)}[\dot{\xi}^r - \gamma(\xi_i - \delta_i - \xi^r)], \end{aligned} \tag{13}$$

where $u = \dot{\xi}$, $\eta_i = \sum_{j=1}^{n+1} a_{ij}$, and $\forall i \neq j$, $\Delta_{ij} = \delta_i - \delta_j$ denotes the difference in the expected information state, and γ is the weight vector.

Define $\tilde{\xi}_i = \xi_i - \delta_i$ and $\tilde{u}_i = u_i - \dot{\delta}_i$. Then, with $\dot{\tilde{\xi}}_i = \tilde{u}_i$, the proof process is similar to the previous Section 2.2.1, just replace ξ_i with $\tilde{\xi}_i$, and u_i with $\tilde{u}_i$. Finally, we can obtain that when $t \longrightarrow \infty$, $\tilde{\xi}_i \longrightarrow \xi^r$, and $\xi_i \longrightarrow \xi^r + \delta_i$.

2.2.3 Group consistency

In the agent system with multiple microwave sources, the introduction of subleaders does not increase the difficulty of the implementation of the control algorithm. In contrast, it can reduce the complexity of control in a system with a large number of agents. Combined with the control law (7) and slightly improved, the two microwave source agent groups can track different reference power curves, respectively, so there are

$$\begin{cases} u_i = \dfrac{1}{\eta_i}\displaystyle\sum_{j=1}^{n} a_{ij}[\dot{\xi}_j - \gamma(\xi_i - \xi_j)] \\ \qquad + \dfrac{1}{\eta_i}a_{i(n+1)}[\dot{\xi}^r - \gamma(\xi_i - \xi^r)], \\ i, j \in G_1, \\ u_i = \dfrac{1}{\eta_i}\displaystyle\sum_{j=1}^{n} a_{ij}[\dot{\xi}_j - \gamma(\xi_i - \xi_j)] \\ \qquad + \dfrac{1}{\eta_i}a_{i(n+1)}[\dot{\xi}_r' - \gamma(\xi_i - \xi_r')], \\ i, j \in G_2, \end{cases} \tag{14}$$

where $\eta_i = \sum_{j=1}^{n+1} a_{ij}$, $\dot{\xi}_r'$ is the derivative of the leader status, and G_1 and G_2 are the number of agent system groups of multiple microwave sources. Proof, as before, is omitted.

2.2.4 Consistency of the agent group with fixed state deviation

The fixed state deviation is introduced into the cooperative output of multiagent groups, that is, group consistency with fixed expected state deviation. This works combines control law (13) and control law (14) to obtain a consistency algorithm with relative expected deviation to coordinate the output power state of each microwave source agent group.

$$\begin{cases} u_i = \dot{\varsigma}_i + \dfrac{1}{\chi_i}\displaystyle\sum_{j=1}^{n} a_{ij}\{\dot{\xi}_j - \dot{\varsigma}_j - \lambda[(\xi_i - \xi_j) - (\varsigma_i - \varsigma_j)]\} \\ \qquad + \dfrac{1}{\chi_i}a_{i(n+1)}[\dot{\xi}^r - \lambda(\xi_i - \varsigma_i - \xi^r)], \qquad i, j \in G_1, \\ u_i = \dot{\varsigma}_i + \dfrac{1}{\chi_i}\displaystyle\sum_{j=1}^{n} a_{ij}\{\dot{\xi}_j - \dot{\varsigma}_j - \lambda[(\xi_i - \xi_j) - (\varsigma_i - \varsigma_j)]\} \\ \qquad + \dfrac{1}{\chi_i}a_{i(n+1)}[\dot{\xi}_r' - \lambda(\xi_i - \varsigma_i - \xi_r')], \qquad i, j \in G_2, \end{cases} \tag{15}$$

where $\chi_i = \sum_{j=1}^{n+1} a_{ij}$, λ is the weight vector, $\Delta_{ij} = \varsigma_i - \varsigma_j$ denotes the difference in the expected information state, and G_1 and G_2 are the numbers of agent system groups of multiple microwave sources. Proof, as before, is omitted.

2.2.5 Algorithm complexity analysis

Let $T(n) = O(f(n))$, call $O(f(n))$ the time complexity of the algorithm, and let $S(n) = S(f(n))$, where $S(f(n))$ is the space complexity of the algorithm. n is the input scale

and $f(n)$ is the auxiliary function. The basic statement of the consistency algorithm in this study is the control law of the innermost loop. There are three loops, two of which have an input scale of n, so the time complexity is $O(n^2)$. The auxiliary space required for the implementation of the algorithm is a constant relative to the amount of input data, so the space complexity is $S(1)$, which meets the engineering requirements.

3 Numerical calculation of the multi microwave source agent system

3.1 Model parameters and boundary conditions

The model selects a cuboid as the reaction chamber, and the medium in the chamber is air. The cavity wall and WR340 waveguide wall are made of copper, the feeding microwave frequency is 2.45 GHz, and the working mode is TE_{10}. The heating starts from the room temperature of 20°C, the heated material is SiC, and the total heating time is 31 s. Nodes 1–6 in the system communication topology represent 6 microwave source agents, whose distribution on the cavity is shown in the 3D geometric model constructed in Figure 1(a) and (b) shows the geometry of the y–z cross section.

The initial input parameter settings in the model are shown in Table 1. The temperature characteristics of each parameter of SiC are as follows, and T represents the temperature of the heated medium at the current moment:

$$\begin{aligned}
\varepsilon'(T) &= -2\times10^{-4}T^2 + 0.4503T + 124.26,\\
\tan\delta(T) &= 5\times10^{-10}T^3 - 9\times10^{7}T^2 + 6\times10^{-4}T + 0.2801,\\
k(T) &= 8\times10^{-5}T^2 - 0.325T + 326.69,\\
C_p(T) &= 4\times10^{-7}T^3 - 17\times10^{-4}T^2 + 2.3729T\\
&\quad + 115.43.
\end{aligned} \tag{16}$$

For electromagnetic boundary conditions, the cavity wall and waveguide are made of copper, which can be regarded as a perfect cavity, and is described by the following formula [9,10,17]:

$$\begin{cases}
\boldsymbol{n}\times\boldsymbol{E} = 0,\\
\boldsymbol{n}\cdot\boldsymbol{B} = 0,
\end{cases} \tag{17}$$

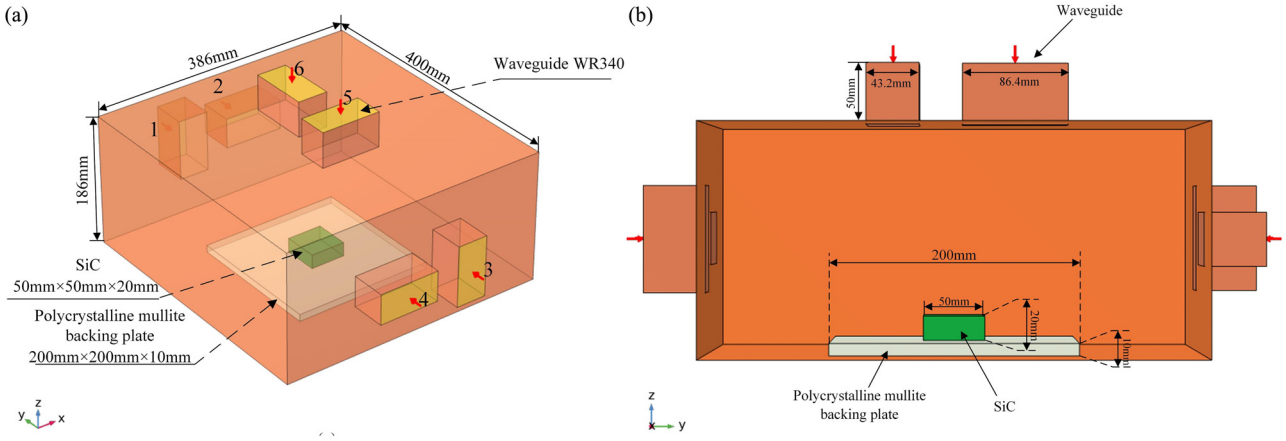

Figure 1: (a) Geometric model of the multisource distributed 3D cavity and (b) geometry of the y–z cross section.

Table 1: Material parameters in the model

materials	Relative permeability	Relative permittivity (real part)	Loss tangent	Electrical conductivity [S·m^{-1}]	Thermal conductivity [W·(m·K^{-1})]	Heat capacity at constant pressure [J·(kg·K^{-1})]	Density [kg·m^{-3}]
SiC[a]	1	$\varepsilon'(T)$	$\tan\delta(T)$	—	$k(T)$	$C_p(T)$	3,100
Copper[a,c]	1	1	—	5.998×10^7	400	3,640	8,700
Air[a,b,c]	1	1	—	0	0	—	—

[a]Reference [32]; [b]Reference [16]; [c]COMSOL built-in material library.

where $\boldsymbol{n}$ denotes the unit normal vector of the cavity wall surface and $\boldsymbol{B}$ is the magnetic induction intensity.

For the heat conduction boundary condition, the natural heat convection between the heated medium and air is expressed as follows [9,28,29]:

$$-k\frac{\partial T}{\partial n} = h \cdot (T - T_{\text{air}}), \tag{18}$$

where $\partial T/\partial n$ denotes the temperature gradient perpendicular to the surface of the temperature domain; h denotes the heat transfer coefficient of air ($10\text{W}\cdot(\text{m}^{-2}\cdot\text{K}^{-1})$); and T_{air} denotes the temperature of air medium inside the reaction chamber. Since the polycrystalline mullite backing plate has excellent heat preservation and wave permeability, its influence on the heating process and the thermal insulation of the contact boundary between the bottom surface of the heated medium and the backing plate surface are ignored [17,28,29]:

$$\boldsymbol{n} \cdot q = 0, \tag{19}$$

where q is the heat flux.

3.2 Model settings

The normalised power absorption (NPA) [16,17,28,29] is introduced to measure the influence of the grid size of the whole geometry on the accuracy of the calculation results. The NPA calculation method used in this model is as follows:

$$\text{NPA} = \frac{\int_0^t \int_V Q_e(\tau)\text{d}V\text{d}\tau}{\int_0^t P(\tau)\text{d}\tau}, \tag{20}$$

where the numerator indicates the absorbed energy of the heated material and the denominator indicates the total energy fed into the system. $Q_e(\tau)$ is the electromagnetic power loss density ($\text{W}\cdot\text{m}^{-3}$) at moment τ, t is the heating time, and $P(\tau)$ is the total feed-in power.

As seen in Figure 2(a), it is concluded that the NPA tends to be stable after the maximum grid size becomes gradually smaller. When the time step is set larger than 0.1 s, the NPA corresponding to different maximum grid sizes is close to 1 or larger than 1, which is clearly incorrect. When the time step setting is less than 0.1 s, the NPA tends to be stable. As seen in Figure 2(b), as the maximum grid size gradually decreases, when the time step setting is less than 0.1 s, the calculation accuracy improves, but the time complexity increases considerably, i.e., the calculation time increases greatly. Therefore, the numerical calculation model in this study selects the maximum grid size of the heated material area as 5 mm, and the time step as 0.1 s.

4 Multi microwave source agent power consistency strategy implementation and results analysis

4.1 Consistency strategy implementation

The system scheme in this work has six microwave source agents with the communication topology set up as shown in Figure 3.

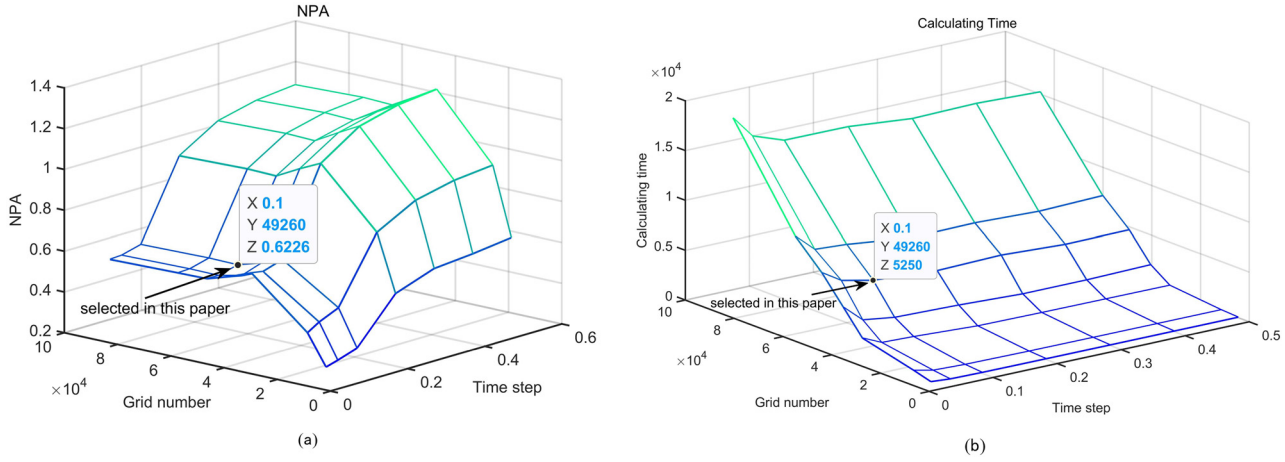

Figure 2: (a) NPA variation with different numbers of grids and time steps and (b) computational time variation with different numbers of grids and time steps.

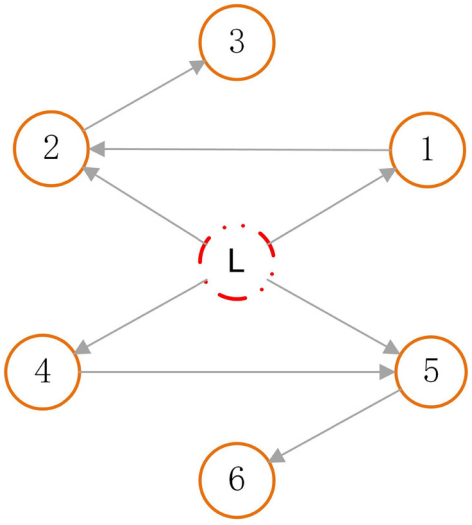

Figure 3: Communication topology of the agent system.

Nodes 1–6 represent the 6 microwave source agents, and the central L node represents the virtual leader, which provides the reference trajectory for the other nodes to track. This topology graph satisfies the consistency algorithm condition.

Based on Figure 3, the adjacency matrix can be obtained as follows:

$$A_{6+1} = \begin{bmatrix} 0 & 0 & 0 & 0 & 0 & 0 & 1 \\ 1 & 0 & 0 & 0 & 0 & 0 & 1 \\ 0 & 1 & 0 & 0 & 0 & 0 & 0 \\ 0 & 0 & 0 & 0 & 0 & 0 & 1 \\ 0 & 0 & 0 & 1 & 0 & 0 & 1 \\ 0 & 0 & 0 & 0 & 0 & 1 & 0 \\ 0 & 0 & 0 & 0 & 0 & 0 & 0 \end{bmatrix}. \tag{21}$$

4.1.1 Basic power consistency strategy

Generally, we let the initial output power (W) of each microwave source agent $\xi_0 = [55, 180, 490, 120, 105, 250]^T$ and the initial input of the system $u_0 = 0_6$. To speed up the convergence, we set the weight vector $K_r = 2_6$. Let the target reference trajectory provided by the virtual leader be the cosine curve $\xi^r = 200(\cos 0.5t + 1)$ and $u_r = \dot{\xi}^r$. The power output is obtained from control law (7) as shown in Figure 4. The consistency algorithm with a nonfully connected fixed topology enables each microwave source agent to effectively track the reference trajectory and collaboratively output consistently varying power values. Additionally, the system state converges consistently after approximately 4.5 s and continues tracking in the subsequent process.

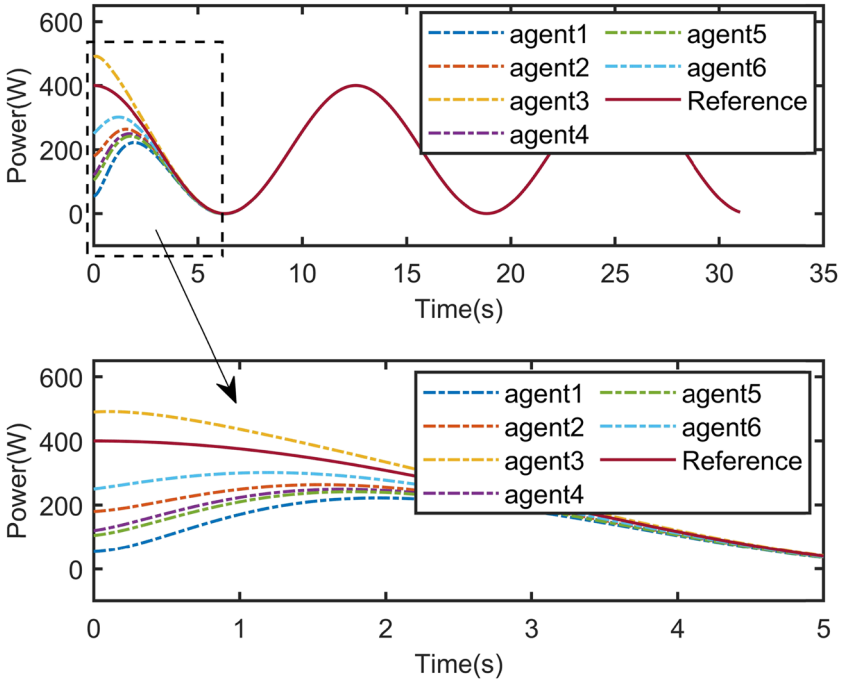

Figure 4: Multi microwave source agent power consistent output.

4.1.2 Analysis of the heating effect of each source

The total energy fed into the reaction chamber in this study is consistent in each experiment and needs to satisfy the following:

$$P_{\text{in}} = \sum_{i=1}^{n} \int_{0}^{t} P_i(\tau)\mathrm{d}\tau, \tag{22}$$

where n denotes the number of excited microwave source agents and $P_i(\tau)$ denotes the power curve of the ith microwave source agents with time τ as the independent variable.

A single microwave source for heating is fed from that source only with a change in power of $P_i(t) = 200(\cos 0.5t + 1)W$, the power fed from other sources is $P_{j,j\neq i} = 0W$, and the heating time is 31 s.

Based on Figure 5, after heating the same material, the overall heating efficiency of the source at various positions and the most affected areas of the heated material are different. Among them, the higher the temperature reached by the material is, the more heat energy it absorbs during the heating process to convert electromagnetic energy, i.e., the higher the absorption efficiency. The ratio of reflected power to feed-in power $|S_{11}|$ [28,29] is introduced to measure the heating efficiency. $|S_{11}|$ can be expressed by equation (23).

$$|S_{11}| = \frac{P_r}{P_{\text{in}}} = \frac{P_{\text{in}} - \int_0^t \int_V Q_e(\tau)\mathrm{d}V\mathrm{d}\tau}{P_{\text{in}}}, \Delta T = T_a - T_0, \tag{23}$$

where P_r is the reflected power, ΔT represents the average temperature rise of the material, T_a is the average temperature of the selected area, T_0 is the initial temperature.

Table 2 shows the reflectivity $|S_{11}|$ of the energy when each microwave source is heated separately. The smaller the $|S_{11}|$ value is, the higher the heating efficiency. Figure 6 shows the trend of the average temperature rise ΔT_{ave} of the heated material and the temperature difference ΔT_{ran} between the highest and lowest temperatures during the heating process of a single microwave source. If the changing waveform of each microwave source is the same, then the energy utilisation rate is not high, which is not conducive to optimising the heating efficiency and energy consumption. Therefore, in the case of the same total input energy, the input power should be different according to the heating efficiency of different microwave sources.

4.1.3 Consistency strategy with a fixed expected power deviation

With the same total energy fed, the power distribution from microwave source 1 to microwave source 6 is as follows:

$$P_i(t) = [105, 165, 105, 280, 245, 300]^T \cdot (\cos 0.5t + 1). \tag{24}$$

When corresponding to the control law (13), the reference power curve takes $\xi^r = \xi_0^r(\cos 0.5t + 1)$, where ξ_0^r is the curve amplitude, $\dot{\xi}^r = u^r$, $\xi_0^r = 100$. The initial output power ξ_0 is consistent with the above, the expected power

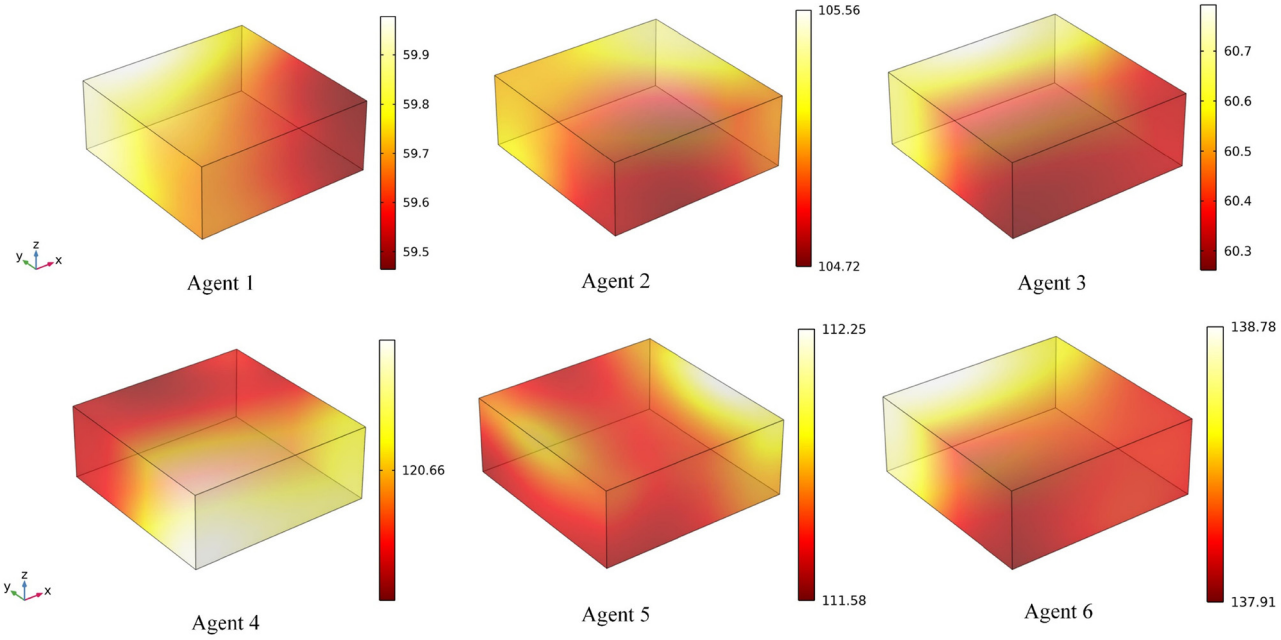

Figure 5: Comparison of the heating effects of each microwave source agent alone.

Table 2: When each microwave source agent is heated individually $|S_{11}|$

Agent number	Agent 1	Agent 2	Agent 3	Agent 4	Agent 5	Agent 6
$\|S_{11}\|$	0.857	0.495	0.854	0.310	0.410	0.244

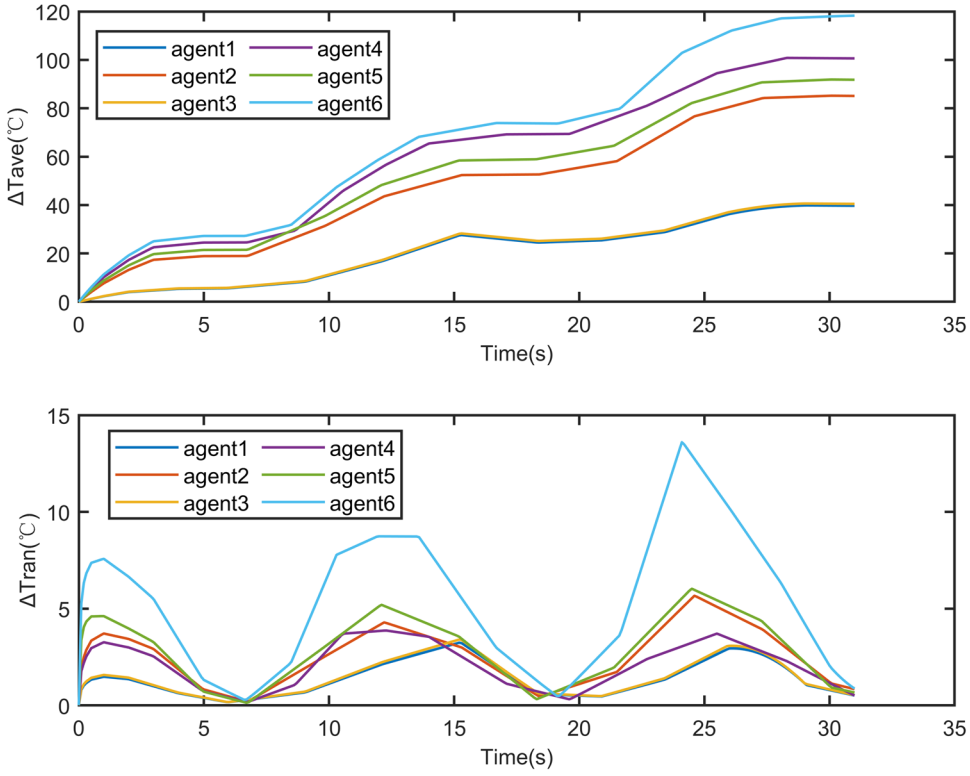

Figure 6: Heating temperature changes at different positions of the distribution of each microwave source agent.

deviation is fixed at $\delta = [10, 130, 10, 360, 290, 400]$, and the system initial input is $u_0 = 0_6$. The weight vector is set at $\gamma = 1_6$ to speed up the convergence and simply increase the weight vector accordingly. The consistent output with power deviation obtained by applying the control law (13) is shown in Figure 7. After approximately 4.7 s, the system state converges to be consistent.

4.1.4 Power consistency strategy of the agent group

According to Figure 6, the microwave source agents with the top three efficiencies form agent group 1, and the others form agent group 2. The two agent groups track different reference power curves. One is $\xi^r = A_1(\cos 0.5t + 1)$, and the other is $\xi_r' = A_2(\cos 0.5(t - \varphi) + 1)$. ξ_r' changes from ξ^r, and φ represents the phase difference. The group communication topology is shown in Figure 8, and the adjacency matrix of this communication topology is consistent with equation (21), where L' is further varied from the virtual leader L.

When the total energy fed into the cavity remains the same, combined with Table 2, the reference power curve of the inefficient agent group is $P_i(t) = 100(\cos 0.5t + 1)W$, $i = 1,2,3$, and the reference power curve of the efficient agent group is $P_i(t) = 300\left(\cos 0.5\left(t - \frac{\pi}{2}\right) + 1\right)W$, $i = 4,5,6$. After using control law (14), the coordinated and consistent power output diagram of the two agent groups of high efficiency and low efficiency, as shown in Figure 9, can be obtained. After approximately 2 s, the system state converges and is consistent.

4.1.5 Agent group consistency strategy with a fixed power deviation

With the total energy fed into the cavity unchanged, the agent group G_1 reference power curve is $\xi^r = A_m(\cos 0.\ 5t + 1)$

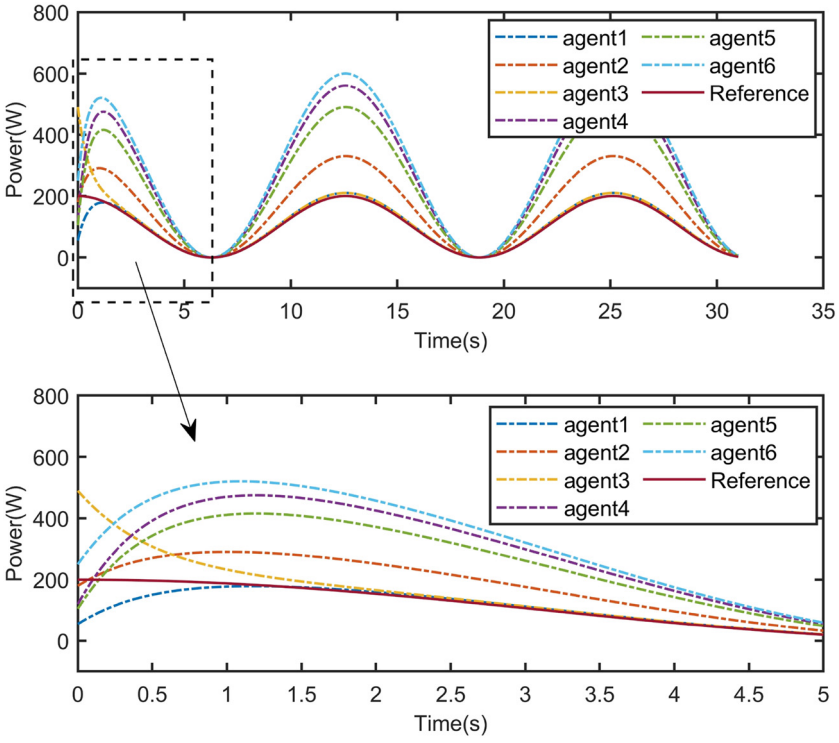

Figure 7: Power consistent output of the microwave source agent with expected power deviation.

and the agent group G_2 reference power curve is $\xi_r' = A_{m1}(\cos(0.5t - \pi/4) + 1)$. The power output distribution of the two agent groups is as follows:

$$\begin{cases} P_i(t) = [105, 155, 105]^T \cdot (\cos 0.5t + 1), & i = 1, 2, 3, \\ P_j(t) = [280, 245, 310]^T \cdot (\cos(0.5t - \pi/4) + 1), & \\ j = 4, 5, 6, & \end{cases} \quad (25)$$

where i and j denote the agent number.

The initial output power ξ_0 remains unchanged, and the expected power deviation of the two agent groups is $\begin{cases} \varsigma_i = [10, \quad 110, \quad 10], i = 1,2,3 \\ \varsigma_j = [360, \quad 290, \quad 420], \quad j = 4,5,6. \end{cases}$ To satisfy the desired power output waveform of formula (25), the initial input of the system is $u_0 = 0_6$, and the weight vector is $\chi = 1_6$ to speed up the convergence and simply increase the weight vector accordingly. Using control law (15), Figure 10 shows the coordinated and consistent power output diagram of two agent groups with a fixed power deviation. After approximately 3.5 s, the system state converges and is consistent.

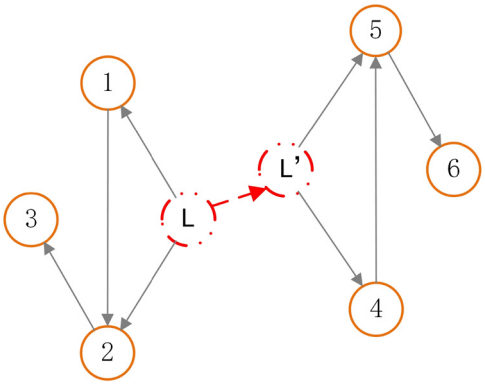

Figure 8: Agent group communication topology.

4.2 Results and analysis

The initial value ξ_0 remains unchanged, and each microwave source agent feeds power according to the four reference power curves mentioned in the study, builds a numerical calculation model, and heats for 31 s. Compared with the traditional multisource constant power heating model, the temperature distribution of the heated material is obtained, as shown in Figure 11.

According to Figure 11, for the heating model using the basic consistency strategy in the experiment, the difference between the highest and lowest temperatures is only 5°C, and the material temperature distribution is substantially better than that of the traditional multisource constant power heating model. However, with traditional multisource heating, the overall temperature rise

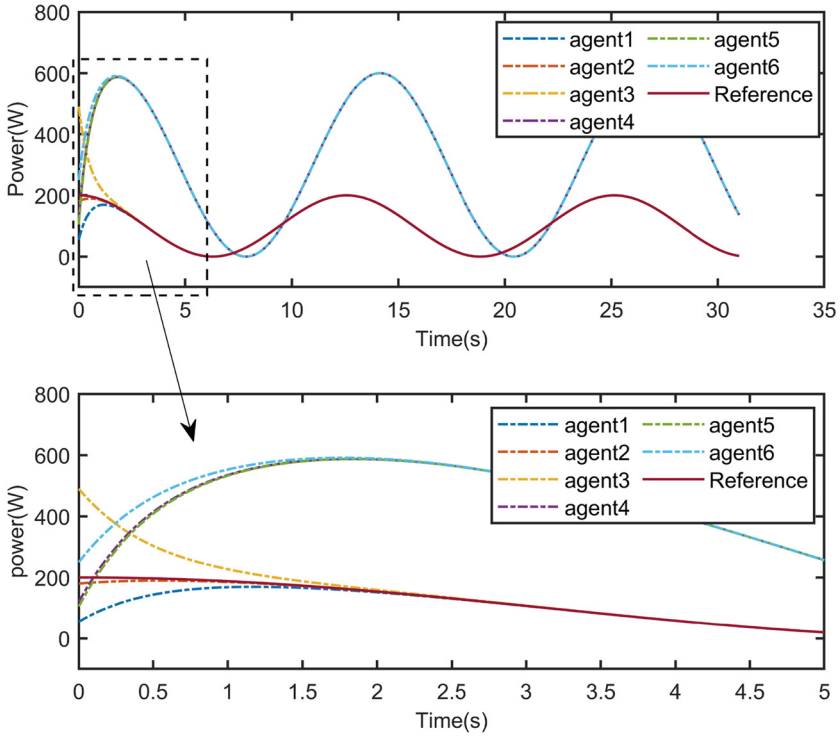

Figure 9: Power consistent output of multi microwave source agent group.

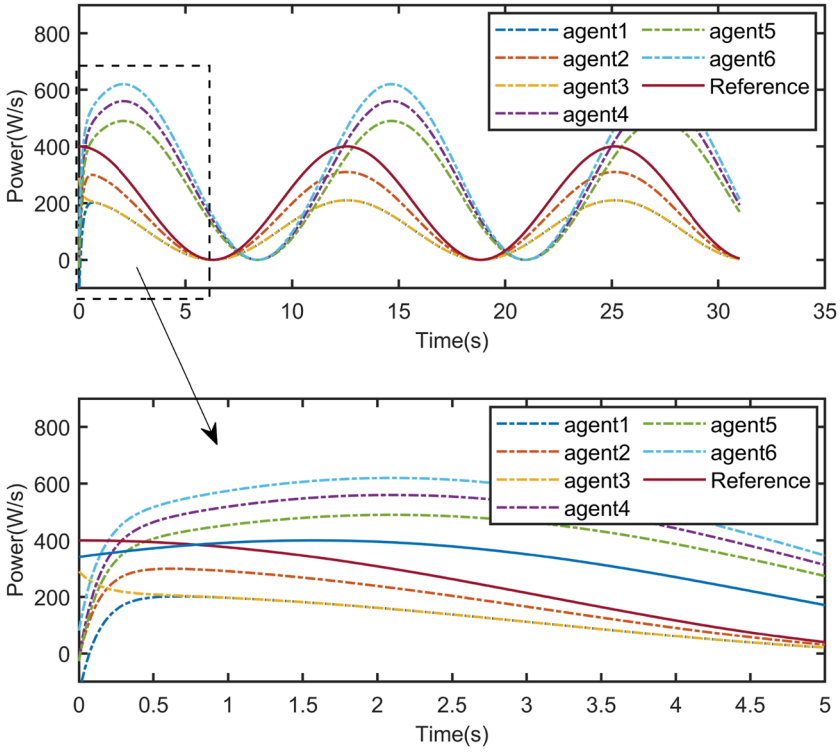

Figure 10: Consistent output of agent group power with expected power deviation.

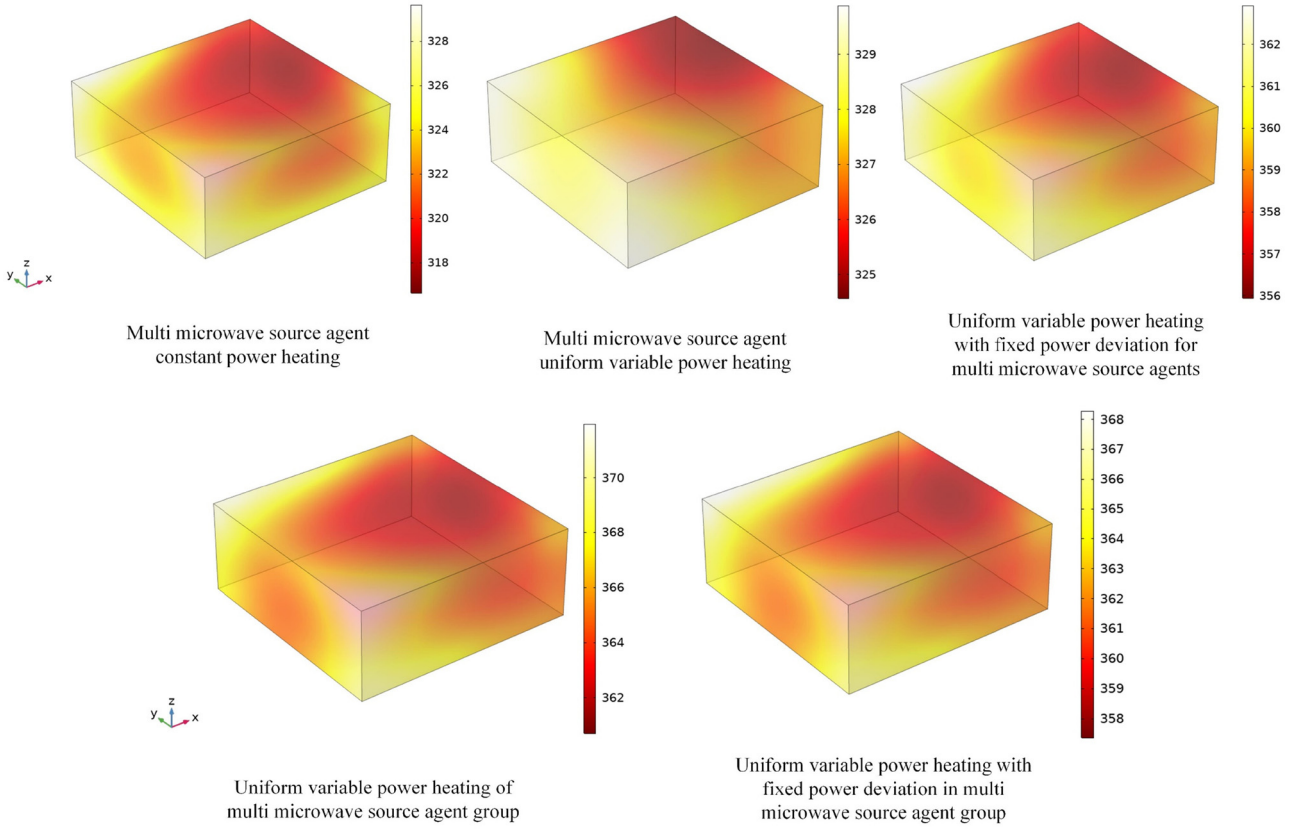

Figure 11: Comparison of the heating effect.

has a small gap, and the heating efficiency is not high. The consistent heating strategy containing a fixed power deviation demonstrates a high overall temperature rise, and its heating efficiency is higher than that of the basic consistent heating strategy. Compared with the above two models, the temperature distribution effect of the

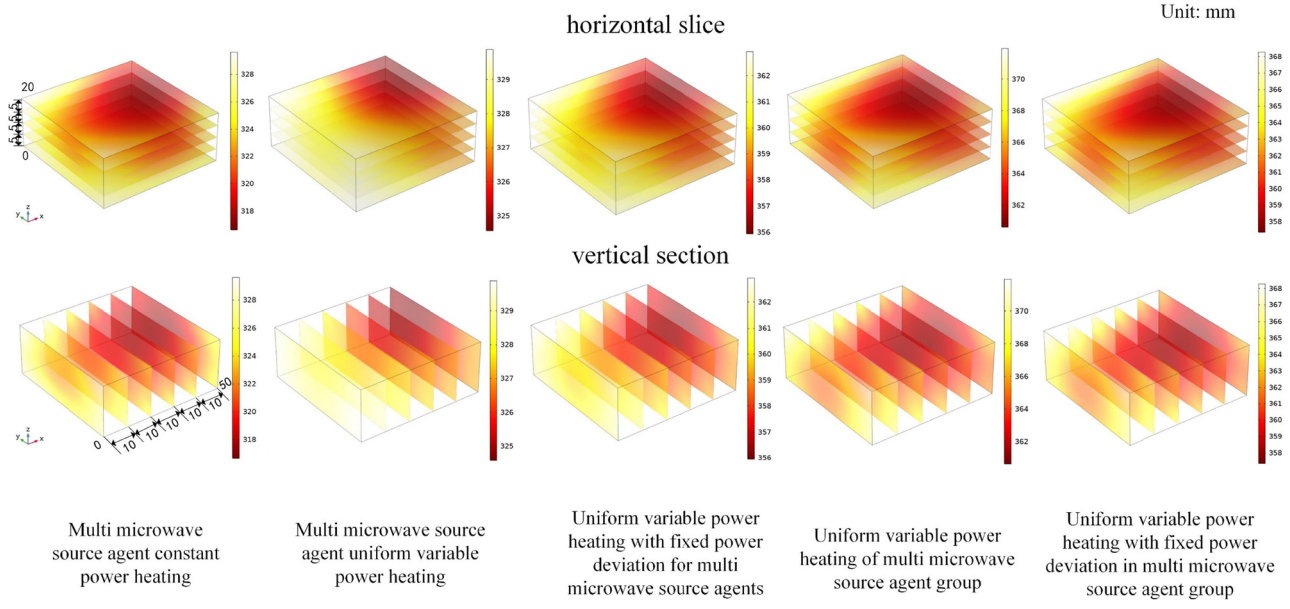

Figure 12: Heating effect section of the five models.

Table 3: Horizontal section COV

Heating category	Section height				
	20 mm	15 mm	10 mm	5 mm	0 mm
Multi-source constant power	0.0115	0.0112	0.0105	0.0109	0.0112
Multi-source consistent variable power	0.0056	0.0057	0.0058	0.0058	0.0057
Consistency with power deviation	0.0058	0.0057	0.0055	0.0056	0.0056
Group consistency	0.0085	0.0080	0.0072	0.0072	0.0073
Group consistency with power deviation	0.0085	0.0080	0.0071	0.0070	0.0071

Table 4: Vertical section COV

Heating category	Section depth					
	0 mm	10 mm	20 mm	30 mm	40 mm	50 mm
Multi-source constant power	0.0072	0.0070	0.0064	0.0060	0.0077	0.0098
Multi-source consistent variable power	0.0017	0.0017	0.0017	0.0022	0.0031	0.0035
Consistency with power deviation	0.0030	0.0027	0.0025	0.0025	0.0030	0.0035
Group consistency	0.0064	0.0062	0.0061	0.0052	0.0049	0.0050
Group consistency with power deviation	0.0060	0.0056	0.0056	0.0053	0.0049	0.0050

agent group consistent heating strategy and the agent group consistent heating strategy with fixed power deviation is slightly worse; however, the maximum temperature of the heated material can reach 370°C, and its heating efficiency is considerably improved. The temperature distribution of the four heating models proposed in this study is better than the multisource constant power heating effect, and it is far better than the single-source heating effect [27].

The temperature coefficient of variation (COV) [9,10,15,16] is introduced to measure the uniformity of the temperature distribution. $|S_{11}|$ and ΔT are introduced to measure the heating efficiency, as shown in Formula (23) above. The COV is represented by equation (26) as follows:

$$\mathrm{COV} = \frac{1}{\Delta T}\sqrt{\frac{1}{n}\sum_{i=1}^{n}(T_i - T_a)^2}, \tag{26}$$

where T_a is the average temperature of the selected area.

Experiments with five different heating methods cut the material horizontally and vertically, as shown in Figure 12, and the COV of each section is calculated. The calculation results are shown in Tables 3 and 4.

As seen in Tables 3 and 4, the heating effect of the four proposed heating models is all better than that of the traditional heating model from the literature [27], and has the smallest COV in each horizontal section and vertical section. That is, the COV values of the models proposed in the study are smaller. In the comparative experiment in this study, the traditional heating model with multiple microwave sources with constant power is added. The power fed into the cavity by each microwave source is 200 W, which is the same as that of industrial microwave heating materials. The uniformity of the horizontal section and vertical section is increased by 26.1–51.3% and 12.5–76.4% respectively, which can considerably improve the heating uniformity. The consistent heating model with the fixed power deviation and the multisource consistent variable power heating model have substantially better heating uniformity than all other heating models. In a limited range, the uniformity of the consistent heating model with fixed power deviation is slightly lower than

Table 5: Different heating models $|S_{11}|$

Heating category	Multi-source constant power	Multi-source consistent variable power	Consistency with power deviation	Group consistency	Group consistency with power deviation
$\lvert S_{11}\rvert$	0.392	0.400	0.263	0.300	0.304

Table 6: Horizontal section ΔT

Heating category	Section height				
	20 mm	10 mm	15 mm	10 mm	0 mm
Multi-source constant power	302.2	301.8	301.3	301.9	302.4
Multi-source consistent variable power	307.2	307.2	307.3	307.3	307.3
Consistency with power deviation	339.1	339.0	338.8	338.9	339.0
Group consistency	345.7	345.2	344.3	344.3	344.4
Group consistency with power deviation	342.2	341.8	341.0	341.0	341.0

Table 7: Vertical section ΔT

Heating category	Section depth					
	0 mm	10 mm	20 mm	30 mm	40 mm	50 mm
Multi-source constant power	305.6	303.9	301.6	299.9	299.3	299.9
Multi-source consistent variable power	309.3	308.8	307.6	306.4	305.7	305.5
Consistency with power deviation	341.2	340.4	339.1	337.9	337.3	337.3
Group consistency	347.6	346.7	345.0	343.3	342.8	343.2
Group consistency with power deviation	344.1	343.0	341.4	340.1	339.5	339.8

that of the multisource consistent variable power heating model. The group consistent heating strategy and the group consistent heating strategy with fixed power deviation do not completely reduce the power at the same time due to the phase difference of the feed power waveform, and thus, the uniformity is slightly worse than the other two heating models proposed in the study; however, compared with the traditional heating model, the heating uniformity is effectively improved. The traditional heating model has poor temperature uniformity, which is not conducive to control. The hot spots of the heated materials have a high randomness, which easily causes difficult problems such as thermal runaway. However, the four heating models mentioned in this study have good optimisation effects, which can avoid such problems and control the material heating well. The four proposed heating models are advantageous mainly because with gradually declining power, the temperature in the hot spot area of the material will spontaneously conduct radially to the relatively low temperature area. At the same time, because feed power still exists, the overall temperature will not fall, and no new hot spots will be generated. This realises the use of the self-organisation characteristics of the temperature distribution to improve the heating uniformity.

Additionally, the $|S_{11}|$ and ΔT of different sections of the five models during the heating process are calculated, and the results are shown in Tables 5–7.

According to Tables 5–7, all four models proposed in this study have smaller $|S_{11}|$ values than the three conventional heating models in the literature [27] throughout the heating process. Except for the multisource consistent variable power heating model having little difference from the traditional multisource constant power heating model proposed in this study, the $|S_{11}|$ of the other three new heating models proposed in this study are much smaller than the $|S_{11}|$ of the traditional heating model. The consistent variable power heating with fixed power deviation exhibits the smallest value, namely, $|S_{11}| = 0.263$. That is, approximately 73.7% of the feed-in power is absorbed and converted into thermal energy with high heating efficiency. Meanwhile, the ΔT of each horizontal section is greater than 338°C, and the ΔT of each vertical section is greater than 337°C, which is higher than that of multisource consistent variable power heating, and is much higher than that of the traditional multisource constant power heating method. In this study, the group-consistent heating strategy and the group-consistent heating strategy with fixed power deviation are proposed after the power distribution of each microwave source agent. Compared with the traditional multisource heating model in this study and the traditional heating model from the literature [27], the thermal energy conversion efficiency of the proposed heating model after the power distribution of each microwave source agent is increased by

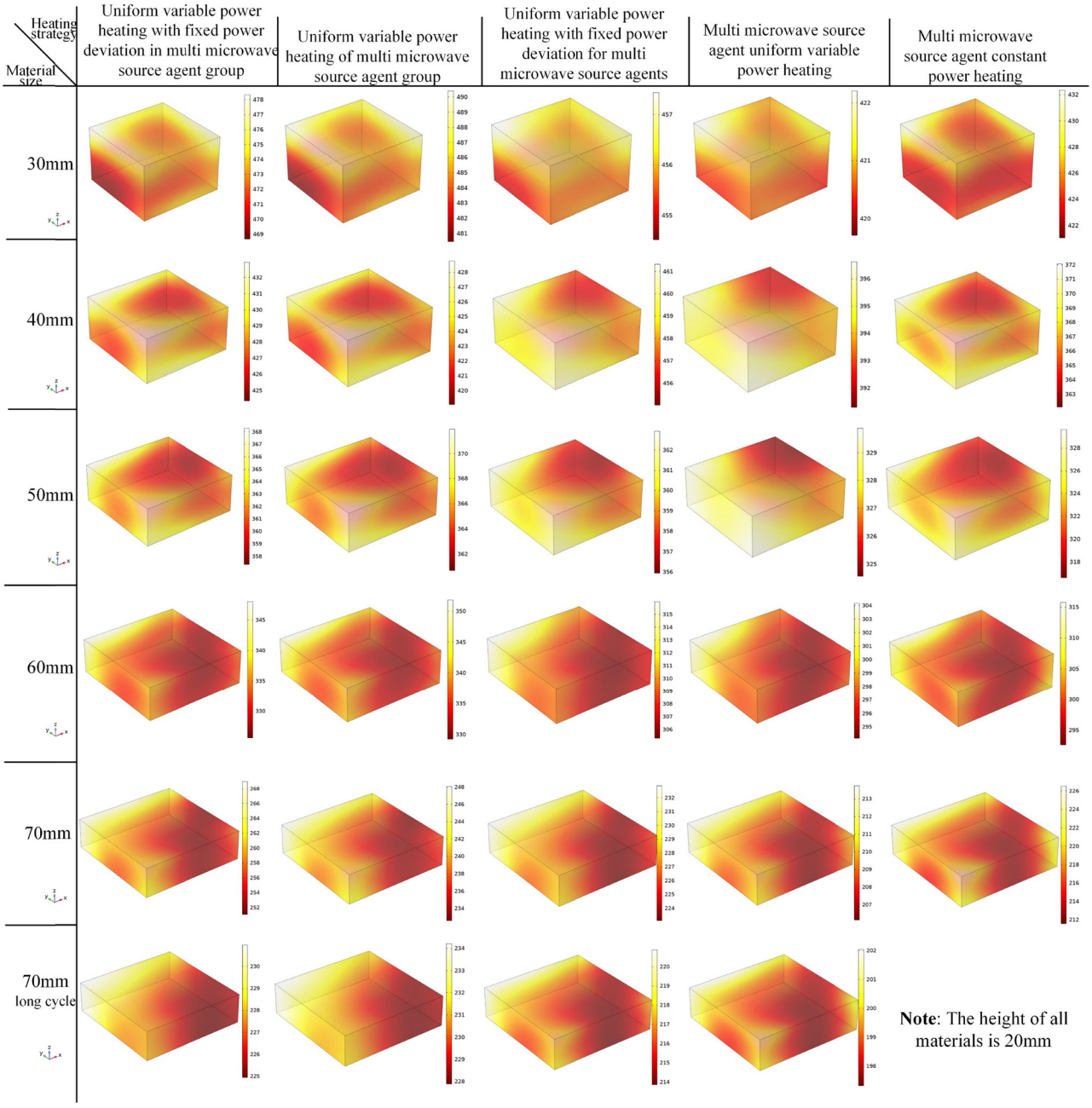

Figure 13: Comparison of the heating effects of materials with different specifications.

23.5–68.2%. Additionally, a comparison with the multisource consistent variable power heating model shows that the thermal energy conversion efficiency is increased by 24–34.3%. The group consistency heating and the group consistency heating with fixed power deviation have a horizontal section ΔT greater than 344°C and a vertical section ΔT greater than 342°C. The highest heating temperature rise reaches 350°C. The heating temperature varies greatly, and the heating efficiency is higher than other heating methods, and it is much higher than the traditional multisource constant power heating and traditional single-source constant power heating models. The main reasons for this are as follows: the temperature distribution in the heating process with changing power is a periodic gentle process, the heating materials at each point of the dielectric coefficient of change are not very different, and sudden changes and thermal runaway do not easily occur. According to the different heating efficiencies of

Table 8: COV on the upper surface of each heating model

Heating category	30 mm	40 mm	50 mm	60 mm	70 mm	70 mm (Long cycle)
Multi-source constant power	0.0052	0.0065	0.0115	0.0185	0.0220	—
Multi-source consistent variable power	0.0010	0.0038	0.0056	0.0095	0.0106	0.0063
Consistency with power deviation	0.0009	0.0035	0.0058	0.0101	0.0132	0.0093
Group consistency	0.0034	0.0048	0.0085	0.0168	0.0189	0.0086
Group consistency with power deviation	0.0035	0.0046	0.0085	0.0172	0.0202	0.0085

Table 9: Different heating models $|S_{11}|$

Heating category	30 mm	40 mm	50 mm	60 mm	70 mm	70 mm (Long cycle)
Multi-source constant power	0.654	0.518	0.392	0.229	0.383	—
Multi-source consistent variable power	0.661	0.527	0.400	0.261	0.413	0.450
Consistency with power deviation	0.586	0.421	0.263	0.214	0.318	0.381
Group consistency	0.587	0.422	0.300	0.226	0.321	0.352
Group consistency with power deviation	0.585	0.420	0.304	0.223	0.318	0.349

microwave sources in various locations, differential power distribution can improve energy utilisation, and thus greatly enhance the heating efficiency.

When the thickness of the heated material is 20 mm and the side lengths are 30, 40, 50, 60, and 70 mm, the different effects of the proposed heating strategy and the traditional heating method are discussed.

As seen in Figure 13, using the multisource constant power heating strategy, the temperature difference between the highest temperature and the lowest temperature of the material is large, while the multisource consistent variable power heating strategy has a small temperature difference change, which can considerably improve the heating uniformity. Using the consistent heating strategy with fixed power deviation, the temperature difference is small, and the maximum temperature of the heated material is much higher than that of the multisource constant power heating strategy, so it can substantially improve the uniformity and heating efficiency. In the group consistency strategy and the group consistency strategy with fixed power deviation, compared with other heating strategies, the overall heating of the material is higher, and the heating efficiency is substantially improved.

As the volume of the heated material increases, the self-organised distribution of the internal temperature of the material requires more time, and the original power change cycle is not enough to make good use of this characteristic. Therefore, the power change cycle is increased to prolong the heat conduction time inside the material. Improved uniformity is compared to the original cycle.

Quantitative analysis of the COV on the upper surface of the material and the overall $|S_{11}|$ are shown in Tables 8 and 9, respectively. As the volume of the heated material increases, the uniformity decreases. The heating uniformity can be considerably optimised by appropriately increasing the power change period. Even if the heated materials have different specifications, compared with the widely used multi microwave source constant power heating, the heating strategy proposed in this study can improve the temperature uniformity and heating efficiency. The above comparative experiments also prove that the heating strategy proposed in this study is scientific and effective.

5 Conclusion and future work

In this work, a nonfully connected communication topology consistency algorithm based on algebraic graph theory is introduced to cooperate with the power feeding state information of multi microwave source agents. At the same time, a new numerical calculation model for cooperative and consistent heating of multi microwave source agents is constructed to study the optimisation of the temperature field distribution in multi microwave source agent system heating.

(1) In this work, based on the intelligence of each microwave source in the process of multisource microwave heating, from the perspective of optimising the electro-

magnetic field distribution in the reaction chamber and the heat conduction in the heating process, the consistency algorithm is applied to achieve the power output coordination of multiple microwave sources. The self-organisation characteristics of the temperature distribution in the heated materials are used to ensure that no new hot spots will be generated, thus improving the temperature uniformity.

(2) According to the different heating efficiencies of microwave sources distributed in various positions of a cavity, a consistency strategy with fixed expected power deviation, a multi microwave source agent group power consistency strategy, and an agent group consistency strategy with fixed power deviation are proposed to improve energy efficiency. The finite element method is used to build a numerical calculation model. An effective calculation to optimise the uniformity of the temperature field distribution and heating efficiency is carried out, and its accuracy and effectiveness are verified by experiments.

The simulation experiment verifies that the multi-source variable power consistent output and the heating model with fixed power deviation consistent output proposed in this work have smaller COVs in the horizontal and vertical sections than other heating models, and the heating uniformity is better. Additionally, the heating model containing a fixed power deviation consistent output is the smallest relative to the other models $|S_{11}|$, and the average heating temperature ΔT for each cross-section is higher than 337°C, which is clearly more advantageous. The heating efficiency of the multi microwave source agent group power consistent output and the agent group consistent output heating model with fixed power deviation is better than all heating models, and the average heating temperature ΔT of each section is the highest. However, the temperature uniformity is slightly lower than that of the heating model proposed in this work in a limited range. Compared with the traditional heating model, the four heating models proposed in this study can improve the temperature uniformity optimisation by 26.1–51.3% and 12.5–76.4% for each level and vertical section, respectively, and the effect is better. In terms of heating efficiency, the heat energy conversion efficiency increases by 23.5–68.2% with more prominent advantages. Finally, by comparing the heating effects of different specifications of materials, the universal applicability of the heating strategy proposed in this study is further verified. The above results show that the new multi microwave source agent system variable power uniform heating model based on the group consistency proposed in this study can improve the temperature uniformity while considerably increasing the heating efficiency.

The limitation of this study is that for the group consistent heating strategy and the group consistent heating strategy with fixed power bias, the heating uniformity is slightly worse than that of the other two new heating strategies proposed in the study. However, since the heating efficiency of the two is much higher than that of the other heating strategies, the qualitative improvement and the slight loss of temperature uniformity are completely acceptable. Moreover, in follow-up research, we will use reinforcement learning and other algorithms to further explore the influence of the phase difference and cycle variation in the virtual leader power curve and the selection of the power deviation value to obtain a better temperature field distribution optimisation effect.

Acknowledgements: The authors gratefully acknowledge the financial supports of the National Natural Science Foundation of China (61863020).

Funding information: National Natural Science Foundation of China (61863020).

Author contributions: Biao Yang: conceptualization, methodology, formal analysis, writing-original draft, writing-review & editing, and funding acquisition. Zhaogang Wu: conceptualization, methodology, formal analysis, writing-original draft, and writing-review & editing. Hao Gao: formal analysis and writing-review &editing. Liexing Zhou, Jun Sun: writing-review & editing.

Conflict of interest: Authors state no conflict of interest.

Data availability statement: All authors can confirm that all data used in this article can be published in High Temperature Materials and Processes.

References

[1] Sun, J., W. L. Wang, and Q. Y. Yue. Review on microwave-matter interaction fundamentals and efficient microwave-associated heating strategies. *Materials*, Vol. 9, No. 4, 2016, id. 231.

[2] Vasudev, H., G. Singh, A. Bansal, S. Vardhan, and L. Thakur. Microwave heating and its applications in surface engineering: a review. *Materials Research Express*, Vol. 6, No. 10, 2019, id. 102001.

[3] Bhattacharya, M., L. Punathil, and T. Basak. A theoretical analysis on the effect of containers on the microwave heating

of materials. *International Communications in Heat and Mass Transfer*, Vol. 82, 2017, pp. 145–153.
[4] Plaza-Gonzalez, P., J. Monzo-Cabrera, J. M. Catala-Civera, and D. Sanchez-Hernandez. Effect of mode-stirrer configurations on dielectric heating performance in multimode microwave applicators. *IEEE Transactions on Microwave Theory and Techniques*, Vol. 53, 2019, pp. 1699–1706.
[5] Wu, Y. P., B. Yan, Y. Yang, H. C. Zhu, and K. M. Huang. Accordion microwave oven for uniformity and efficiency heating. *International Journal of RF and Microwave Computer-Aided Engineering*, Vol. 30, No. 6, 2020, id. e22190.
[6] Geedipalli, S. S. R., V. Rakesh, and A. K. Datta. Modeling the heating uniformity contributed by a rotating turntable in microwave ovens. *Journal of Food Engineering*, Vol. 82, No. 3, 2007, pp. 359–368.
[7] Topcam, H., O. Karatas, B. Erol, and F. Erdogdu. Effect of rotation on temperature uniformity of microwave processed low-high viscosity liquids: A computational study with experimental validation. *Innovative Food Science & Emerging Technologies*, Vol. 60, 2020, id. 102306.
[8] Meng, Q., J. Q. Lan, T. Hong, and H. C. Zhu. Effect of the rotating metal patch on microwave heating uniformity. *Journal of Microwave Power and Electromagnetic Energy*, Vol. 52, No. 2, 2018, pp. 94–108.
[9] Ye, J. H., T. Hong, Y. Y. Wu, L. Wu, Y. H. Liao, H. C. Zhu, et al. Model stirrer based on a multi-material turntable for microwave processing materials. *Materials*, Vol. 10, No. 2, 2017, id. 95.
[10] Liao, Y. H., J. Q. Lan, C. Zhang, T. Hong, Y. Yang, K. M. Huang, et al. A phase-shifting method for improving the heating uniformity of microwave processing materials. *Materials*, Vol. 9, No. 5, 2016, id. 309.
[11] Zhu, H. C., J. B. He, T. Hong, Q. Z. Yang, Y. Wu, Y. Yang, et al. A rotary radiation structure for microwave heating uniformity improvement. *Applied Thermal Engineering*, Vol. 141, 2018, pp. 648–658.
[12] Zhao, H. F., H. Li, X. G. Li, and X. Gao. Process intensification for improving the uniformity and efficiency of microwave heating reactor by bubbles-enhanced flow method. *Applied Thermal Engineering*, Vol. 197, 2021, id. 117346.
[13] Antonio, C. and R. T. Deam. Comparison of linear and non-linear sweep rate regimes in variable frequency microwave technique for uniform heating in materials processing. *Journal of Materials Processing Technology*, Vol. 169, No. 2, 2005, pp. 234–241.
[14] Campanone, L. A., J. A. Bava, and R. H. Mascheroni. Modeling and process simulation of controlled microwave heating of foods by using of the resonance phenomenon. *Applied Thermal Engineering*, Vol. 73, No. 1, 2015, pp. 914–923.
[15] Boonthum, D., S. Chanprateep, C. Ruttanapun, and M. Nisoa. Development of high-temperature multi-magnetron microwave furnace for material processing. *Songklanakarin Journal of Science and Technology*, Vol. 41, No. 3, 2019, pp. 494–500.
[16] He, J. L., Y. Yang, H. C. Zhu, K. Li, W. Yao, and K. M. Huang. Microwave heating based on two rotary waveguides to improve efficiency and uniformity by gradient descent method. *Applied Thermal Engineering*, Vol. 178, 2020, id. 115594.
[17] Xiong, G. C., H. C. Zhu, K. M. Huang, Y. Yang, Z. P. Fan, and J. H. Ye. The impact of pins on dual-port microwave heating uniformity and efficiency with dual frequency. *Journal of Microwave Power and Electromagnetic Energy*, Vol. 54, No. 2, 2020, pp. 83–98.
[18] Ahn, S. H. and W. S. Lee. Uniform microwave heating system design and evaluation with an orthogonally slot-loaded array waveguide. *Microwave and Optical Technology Letters*, Vol. 62, No. 11, 2020, pp. 3419–3424.
[19] Zhou, X. B., H. J. Ma, J. G. Gu, H. L. Chen, and W. Deng. Parameter adaptation-based ant colony optimization with dynamic hybrid mechanism. *Engineering Applications of Artificial Intelligence*, Vol. 114, 2022, id. 105139.
[20] Yao, R., C. Guo, W. Deng, and H. M. Zhao. A novel mathematical morphology spectrum entropy based on scale-adaptive techniques. *ISA Transactions*, Vol. 126, 2022, pp. 691–702.
[21] Zhao, H. M., J. Liu, H. Y. Chen, J. Chen, Y. Li, J. J. Xu, et al. Intelligent diagnosis using continuous wavelet transform and Gauss convolutional deep belief network. *IEEE Transactions on Reliability*, Vol. 47, 2022, pp. 1–11.
[22] Chen, H. Y., F. Miao, Y. J. Chen, Y. J. Xiong, and T. Chen. A hyperspectral image classification method using multifeature vectors and optimized KELM. *IEEE Journal of Selected Topics in Applied Earth Observations and Sensing*, Vol. 14, 2021, pp. 2781–2795.
[23] Wang, G. Distributed control of higher-order nonlinear multi-agent systems with unknown non-identical control directions under general directed graphs. *Automatica*, Vol. 110, 2019, id. 108559.
[24] Li, G. L., C. E. Ren, and C. L. P. Chen. Preview-based leader-following consensus control of distributed multi-agent systems. *Information Sciences*, Vol. 559, 2021, pp. 251–269.
[25] Wu, H., B. R. An, and B. Li. Distributed consensus control protocols for heterogeneous multi-agent systems with time-varying topologies. *IEEE Access*, Vol. 8, No. 2, 2020, pp. 152772–152779.
[26] Wang, K. P., D. Ding, Z. Tang, and J. W. Feng. Leader-following consensus of nonlinear multi-agent systems with hybrid delays: Distributed impulsive pinning strategy. *Applied Mathematics and Computation*, Vol. 424, 2022, id. 127031.
[27] Yang, B., H. Gao, X. P. Li, C. Cheng, W. Du, C. Liu, et al. Research on temperature uniformity optimization of multi-source microwave heating based on consistency theory. *Control and Decision*, Vol. 31, 2022, pp. 1–10.
[28] Zhou, J., X. Q. Yang, J. H. Ye, H. C. Zhu, J. P. Yuan, X. Li, et al. Arbitrary Lagrangian-Eulerian method for computation of rotating target during microwave heating. *International Journal of Heat and Mass Transfer*, Vol. 134, 2019, pp. 271–285.
[29] Zhang, M., X. Jia, Z. Tang, Y. Zeng, X. Wang, Y. Liu, et al. A fast and accurate method for computing the microwave heating of moving objects. *Applied Sciences*, Vol. 10, No. 8, 2020, id. 2985.
[30] Ren, W. Second-order consensus algorithm with extensions to switching topologies and reference models. *Proceedings of the American Control Conference*, New York, NY, 2007, pp. 385–390.
[31] Ren, W. and R. W. Beard. *Distributed Consensus in Multi-vehicle Cooperative Control*, Springer, London, 2008.
[32] Tamang, S. and S. Aravindan. 3D numerical modelling of microwave heating of SiC susceptor. *Applied Thermal Engineering*, Vol. 162, 2019, id. 114250.